

Supporting Information

Ulcerative Colitis Alleviation of Colon-Specific Delivered Rhamnolipid/Fullerene Nanocomposite via Dual Modulation in Oxidative Stress and Intestinal Microbiome

Yuxuan Xia,^a Liu Hong^{*a}, Jiayao Zheng,^a Ziyi Lu,^a Qiong Zhang,^a Siyu Chen,^a Zhi Pang,^{b,c} Lei Li,^d Shumiao Qiao,^e Qiang Wang,^e Yonghua Zhou^{*e} and Cheng Yang^a

^a *Key Laboratory of Synthetic and Biological Colloids, Ministry of Education, School of Chemical and Material Engineering, Jiangnan University, Wuxi 214122, China*

^b *Department of Digestive Disease and Nutrition Research Center, The Affiliated Suzhou Hospital of Nanjing Medical University, Suzhou Municipal Hospital, Gusu School, Nanjing Medical University, Suzhou 215008, China*

^c *Department of Gastroenterology, The Affiliated Suzhou Hospital of Nanjing Medical University, Suzhou Municipal Hospital, Gusu School, Nanjing Medical University, Suzhou 215008, China*

^d *Wuxi School of Medicine, Jiangnan University, Wuxi 214122, China*

^e *Key Laboratory of National Health Commission on Parasitic Disease Control and Prevention, Jiangsu Provincial Key Laboratory on Parasite and Vector Control, Jiangsu Institute of Parasitic Diseases and Public Health Research Center of Jiangnan University, Wuxi 214064, China*

Contents

1. Structure determination of RL/C₆₀

Fig. S1. FT-IR spectrum of RL/C₆₀

Fig. S2. UV-visible absorption spectra of C₆₀, RL and RL/C₆₀

Fig. S3 TGA plots of RL/C₆₀ as tested in N₂

Table S1 Estimation of RL/C₆₀ composition based on TGA data

2. Biocompatibility and antioxidant capacity of RL/C₆₀

Fig. S4 Radical scavenging ability of RL/C₆₀ with different concentrations

3. pH responsive behavior of RL/C₆₀

Fig. S5 Stability of RL/C₆₀ at different pH conditions as shown by FT-IR spectra

Fig. S6 Zeta potential of RL/C₆₀ at different pH conditions

Fig. S7 Visual depiction of RL/C₆₀ release behavior at different pH conditions

4. Evaluation of anti-inflammatory performance of RL/C₆₀

Fig. S8 *In-vitro* antioxidant capacity of RL/C₆₀

Fig. S9 Anatomical photograph of typical mice in different groups

Fig. S10 Daily mice body weight of different groups

Table S2 DAI scoring criteria

Fig. S11 Comparative diagram of mice colon length in different groups

Fig. S12 Th1 and Th2 cells in splenocytes

Fig. S13 Colon-targeted delivery of FITC-labeled RL/C₆₀

5. Modulation effect of RL/C₆₀ on the composition of intestinal microbiota

Fig. S14 PoCA diagram of intestinal microflora (phylum level) from different groups

Fig. S15 Intestinal bacteria community heatmap analysis

Fig. S16 Comparison of group differences in microflora at phylum level

Fig. S17 Potential pathogenic histogram of microbiome in different groups predicted by BugBase

Fig. S18 RL/C₆₀ promotes probiotics colonization while suppresses harmful bacteria proliferation

6. Intestinal flora-immunity relationship and its implication on UC treatment

Fig. S19 Correlation heatmap of inflammatory indicators vs. microflora at genus level

Table S4 SCFAs content in intestinal feces of mice in different groups

1. Structure determination of RL/C₆₀

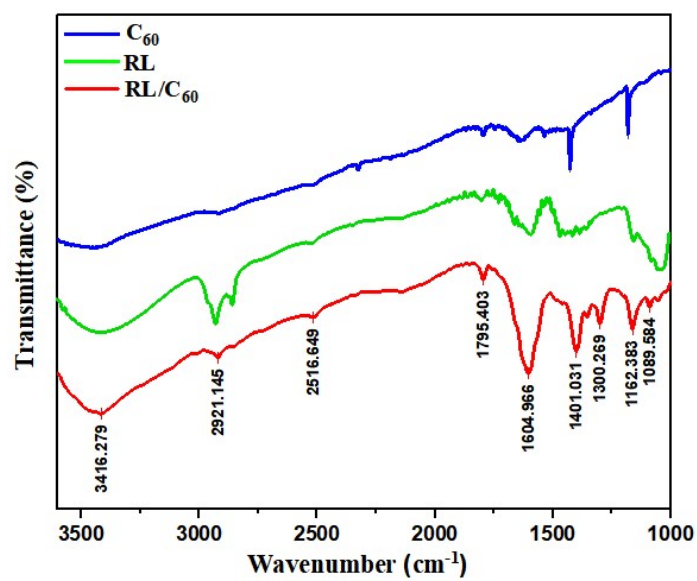


Fig. S1 FT-IR spectrum of C₆₀, RL and RL/C₆₀.

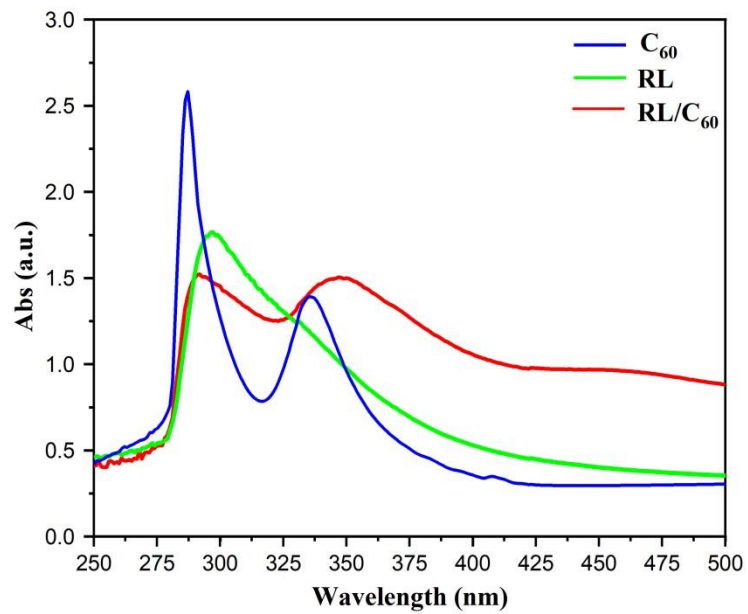


Fig. S2 UV-visible absorption spectra of C₆₀, RL and RL/C₆₀.

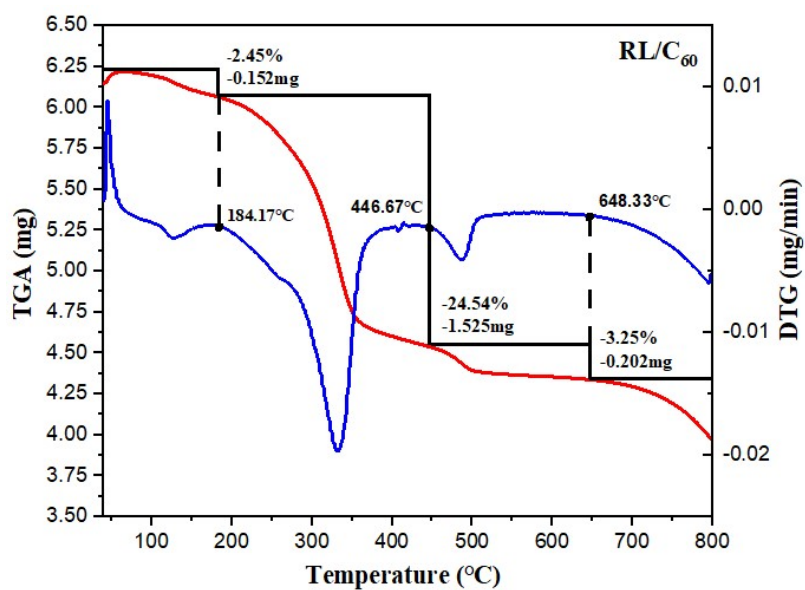


Fig. S3 TGA plots of RL/C₆₀ as tested in N₂.

Table S1 Estimation of RL/C₆₀ composition based on TGA data

Sample	Weight loss (%)			M_{RL}	M_{H_2O}
	y_1	y_2	y_3		
	2.45	24.54	73.01		
RL/C ₆₀	$N_{H_2O} = (720 * y_1) / (M_{H_2O} * y_3)$		$N_{RL} = (720 * y_2) / (M_{RL} * y_3)$	N_{C60}	
	1.34		0.48	1	

2. Biocompatibility and antioxidant capacity of RL/C₆₀

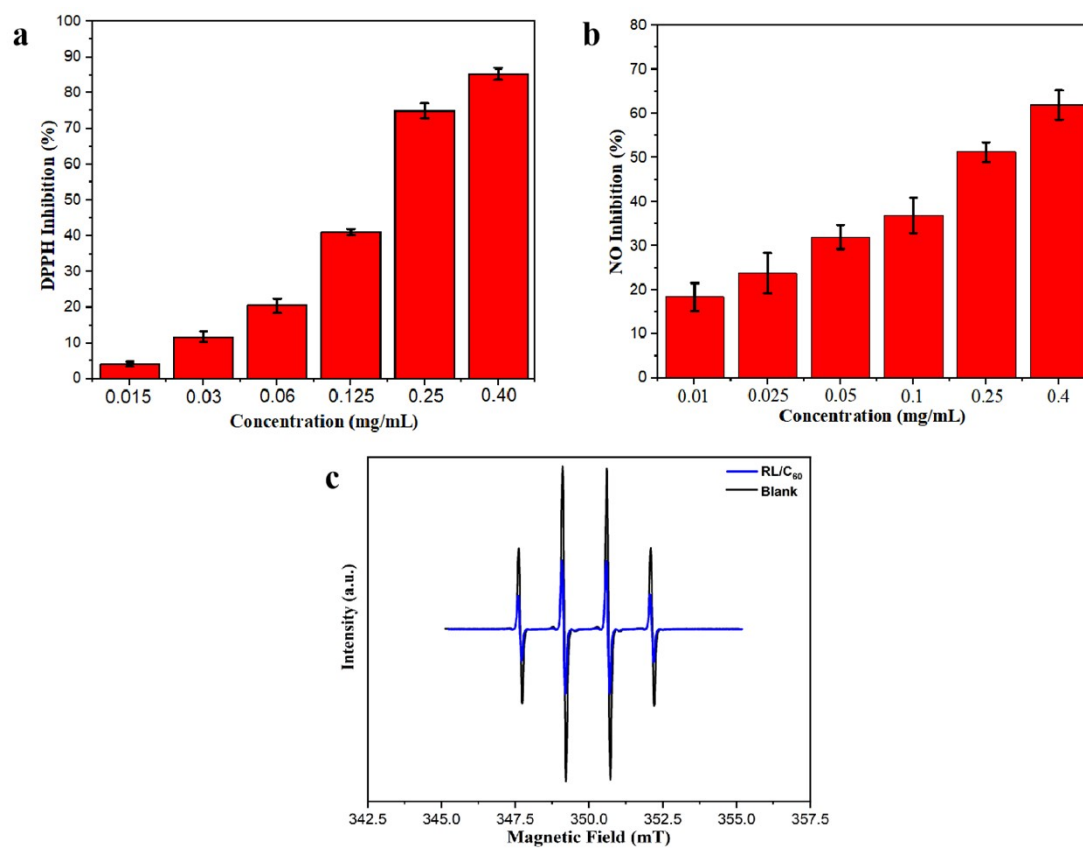


Fig. S4 Radical scavenging ability of RL/C₆₀ with different concentrations: (a) DPPH radical (0.015~0.4 mg/mL); (b) ·NO (0.015~0.4 mg/mL); (c) ·OH (0.4 mg/mL).

3. pH responsive behavior of RL/C₆₀

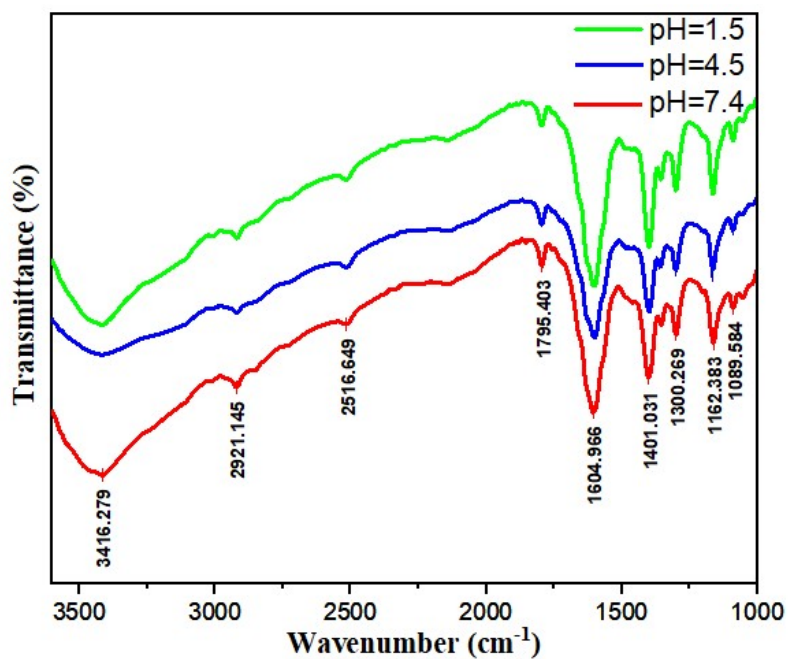


Fig. S5 Stability of RL/C₆₀ at different pH conditions as shown by FT-IR spectra.

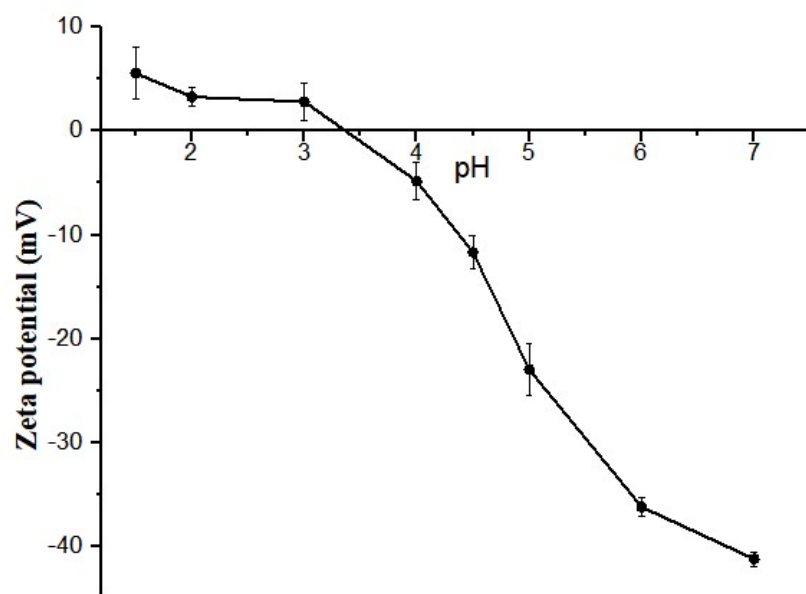


Fig. S6 Zeta potential of RL/C₆₀ at different pH conditions

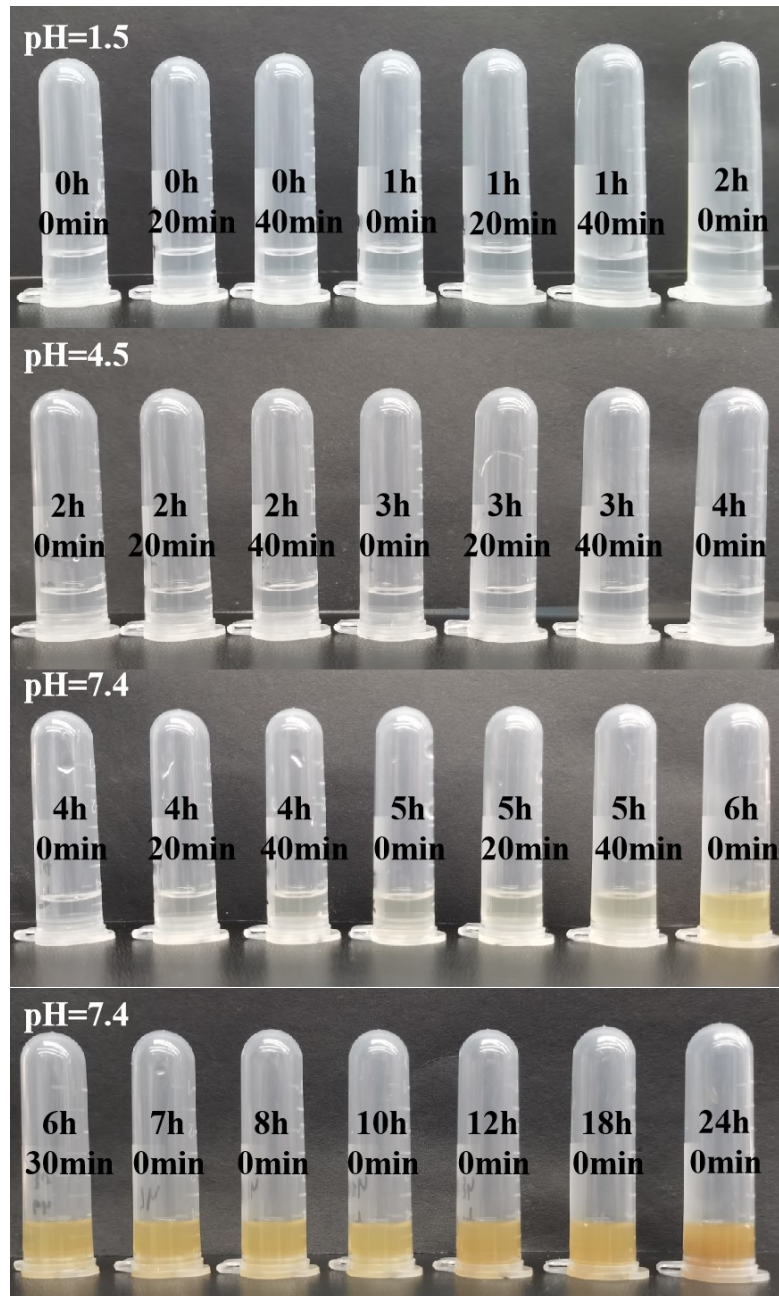


Fig. S7 Visual depiction of RL/C₆₀ release behavior at different pH conditions.

4. Evaluation of anti-inflammatory performance of RL/C₆₀

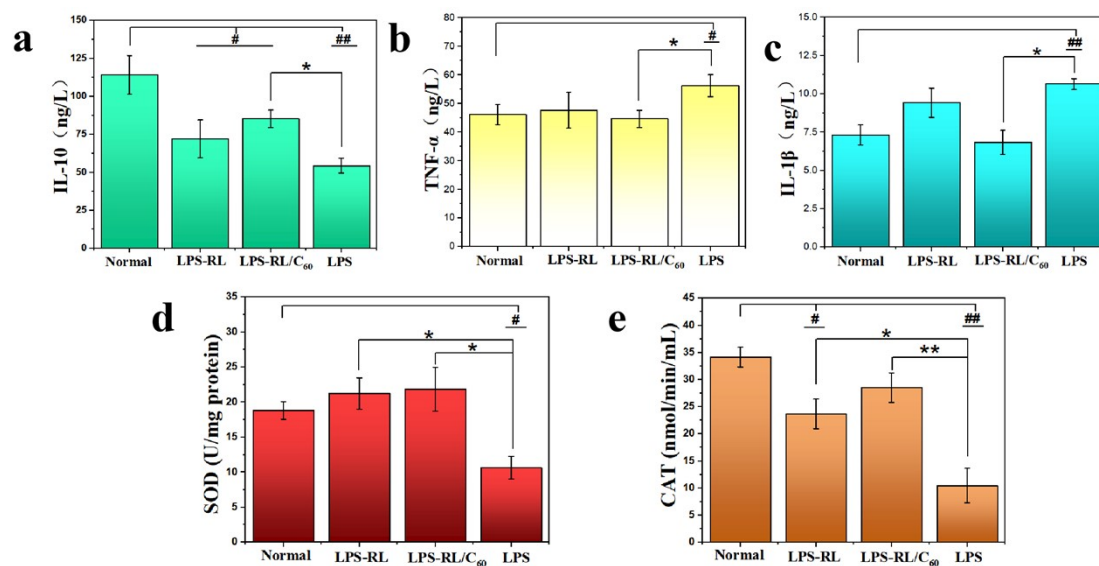


Fig. S8 *In-vitro* antioxidant capacity of RL/C₆₀: (a) IL-10, (b) TNF- α , (c) IL-1 β , (d) SOD, (e) CAT. Data are shown as the mean \pm S.E.M. ($n = 3$). Statistical significance was evaluated via one-way ANOVA with Tukey Test. # $P \leq 0.05$, ## $P \leq 0.01$ vs Normal; * $P \leq 0.05$, ** $P \leq 0.01$ vs LPS.

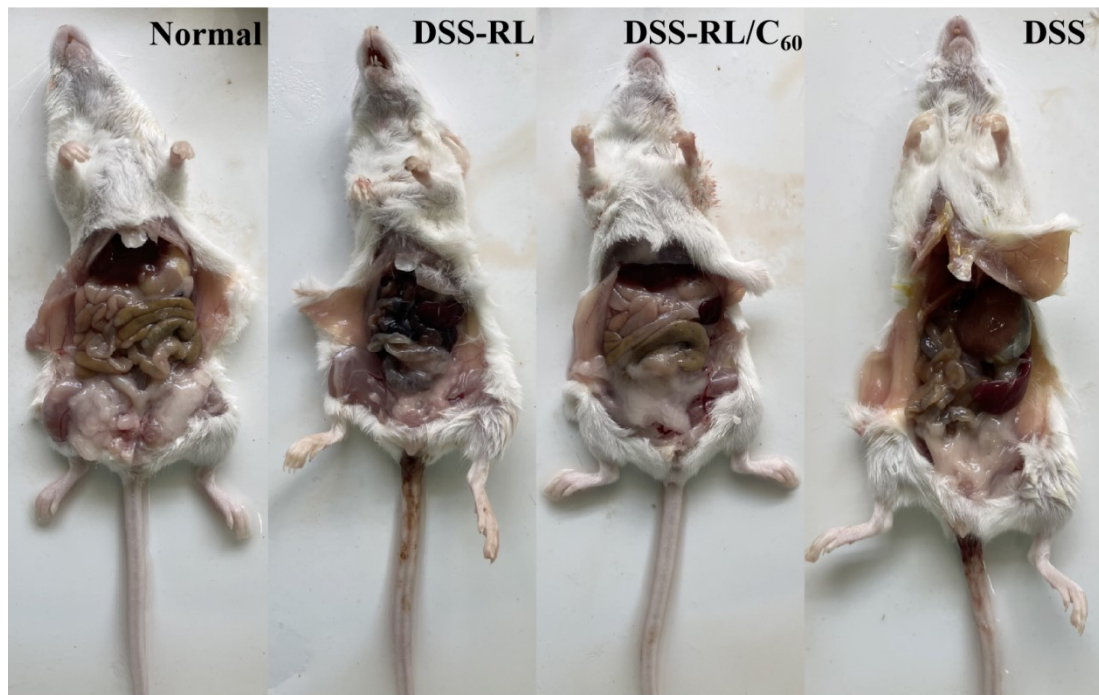


Fig. S9 Anatomical photograph of typical mice in different groups.

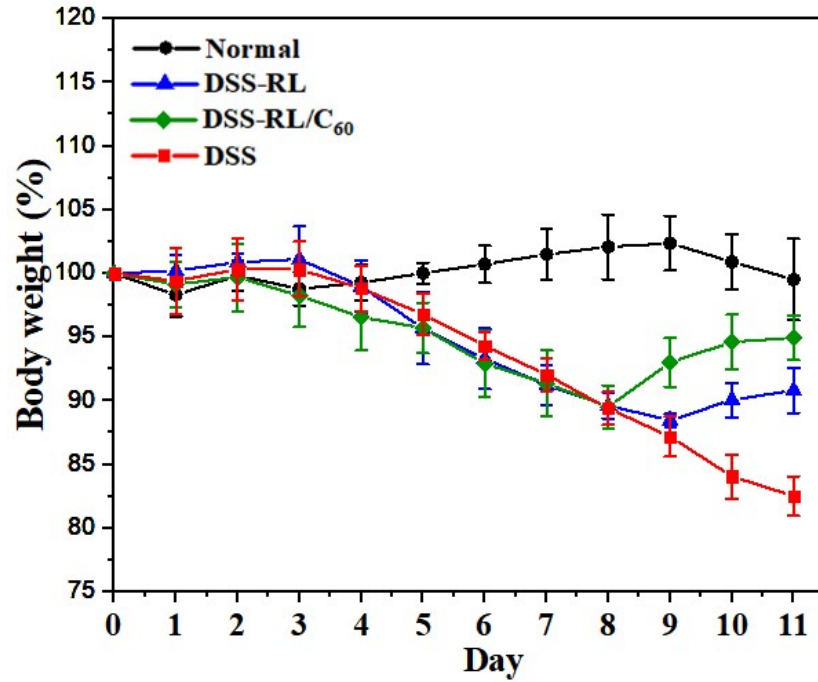


Fig. S10 Daily mice body weight of different groups. Data are shown as the mean \pm S.E.M. ($n = 4$).

Table S2 DAI scoring criteria

Score	Weight Loss (%)	Stool Condition	Hematochezia
0	$X < 2$	normal	no rectal bleeding
1	$2 \leq X < 5$	softer stool	weak hemocult
2	$5 \leq X < 10$	moderate diarrhea	visual blood in stool
3	$10 \leq X < 15$	diarrhea	fresh rectal bleeding
4	$X \geq 15$	/	/

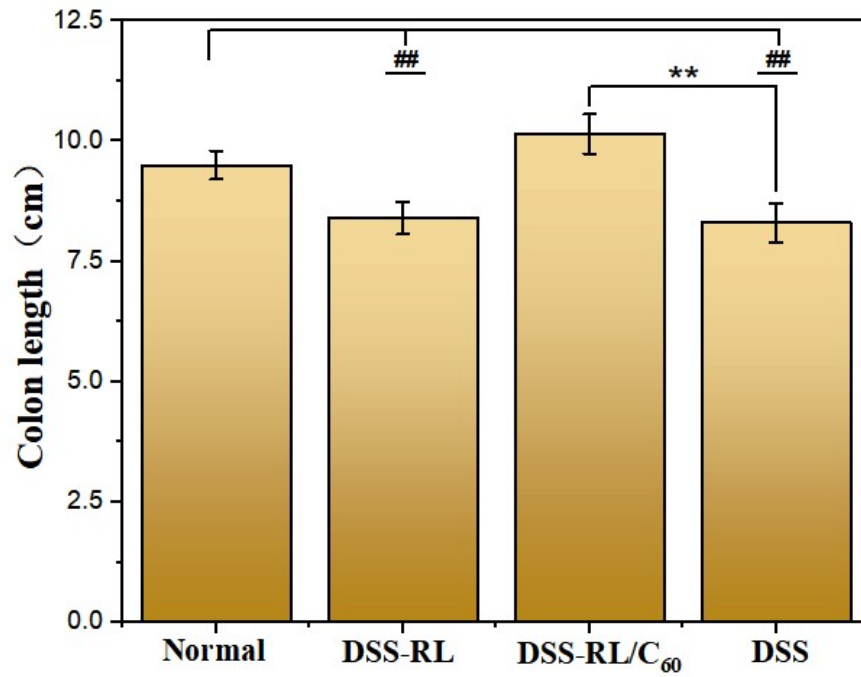


Fig. S11 Comparative diagram of mice colon length in different groups. Data are shown as the mean \pm S.E.M. ($n = 4$). Statistical significance was evaluated via one-way ANOVA with Tukey Test. # $P \leq 0.05$, ## $P \leq 0.01$ vs Normal; ** $P \leq 0.01$ vs DSS.

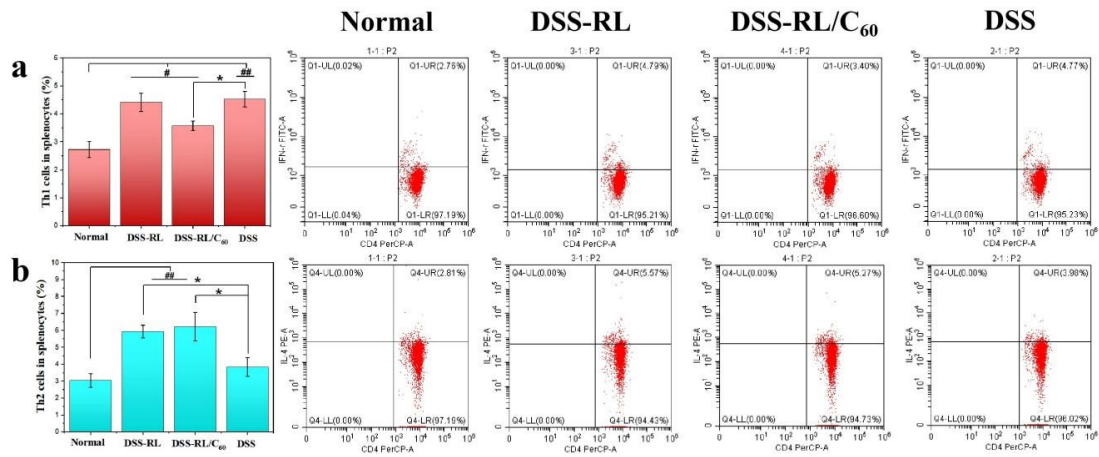


Fig. S12 Th1 and Th2 cells in splenocytes and corresponding flow cytometry data: (a) Th1 cells; (b) Th2 cells. Data are shown as the mean \pm S.E.M. ($n = 4$). Statistical significance was evaluated via one-way ANOVA with Tukey Test. # $P \leq 0.05$, ## $P \leq 0.01$ vs Normal; * $P \leq 0.05$ vs DSS.

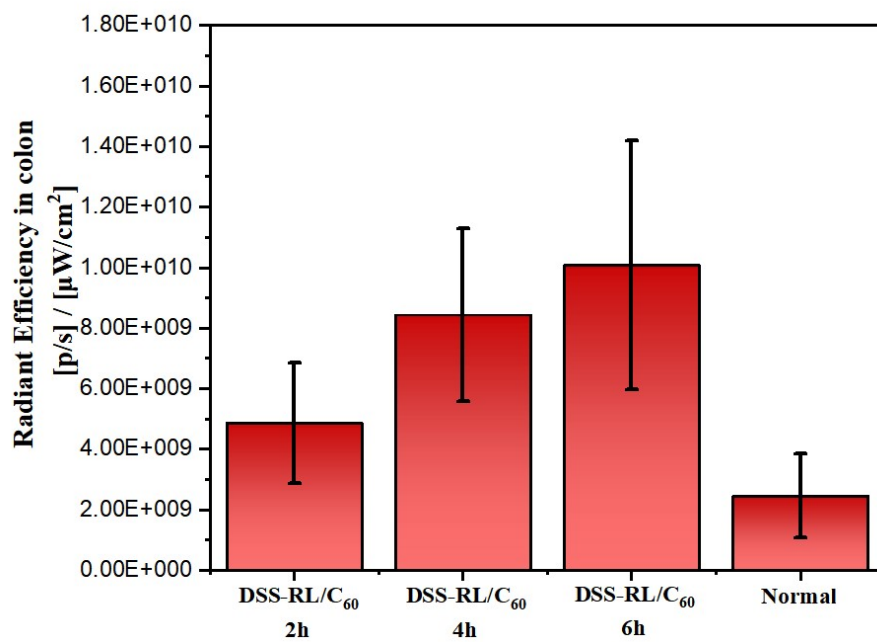


Fig. S13 Colon-targeted delivery of FITC-labeled RL/C₆₀. Data are shown as the mean ± S.E.M. (n = 4).

5. Modulation effect of RL/C₆₀ on the composition of intestinal microbiota

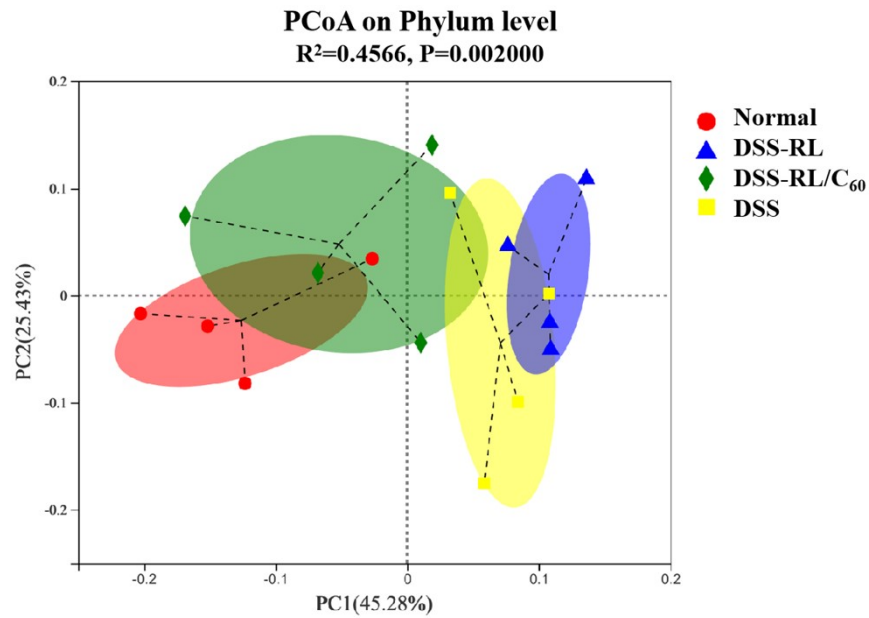


Fig. S14 PoCA diagram of intestinal microflora (phylum level) from different groups.

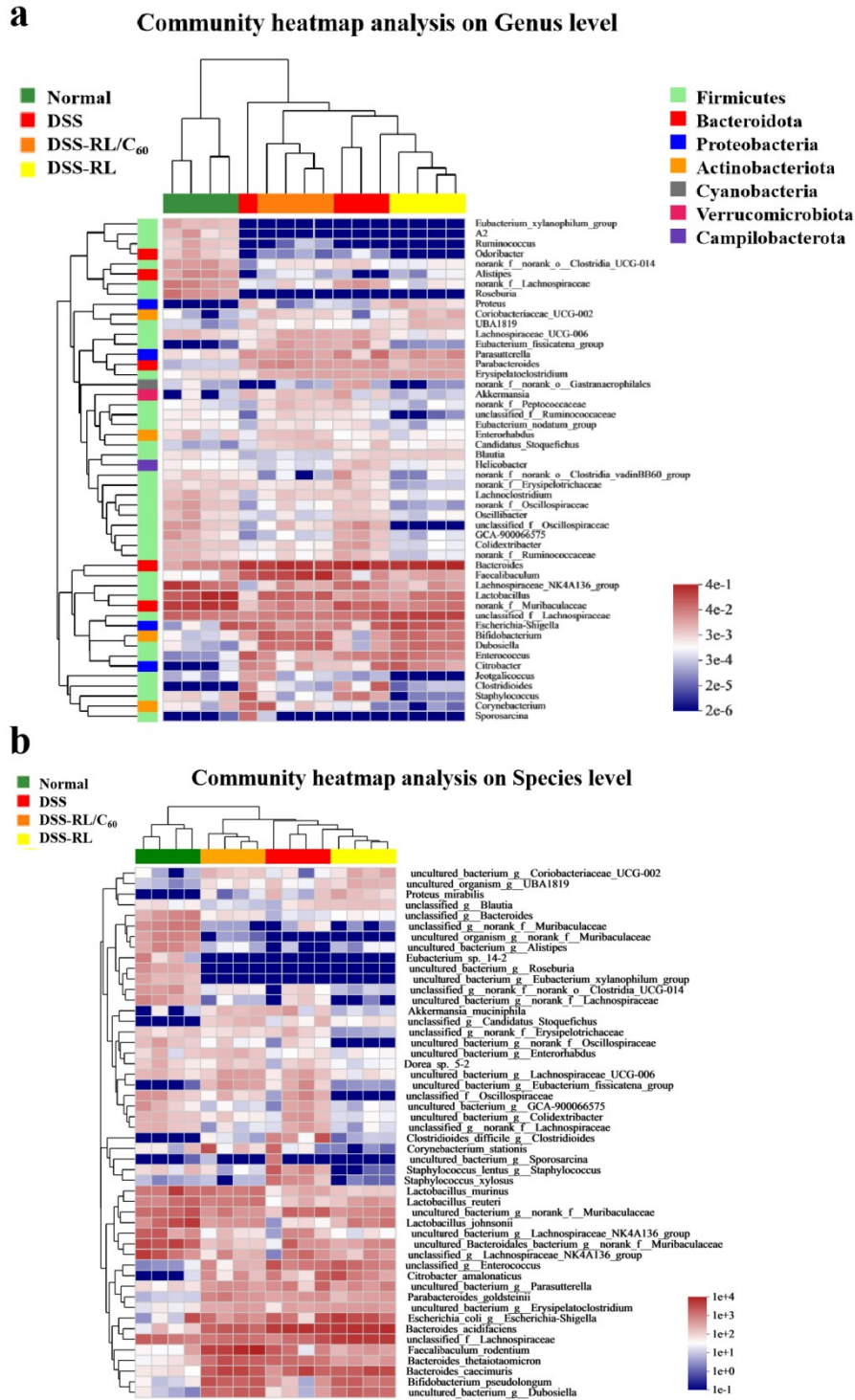


Fig. S15 Intestinal bacteria community heatmap analysis: (a) genus level; (b) species level.

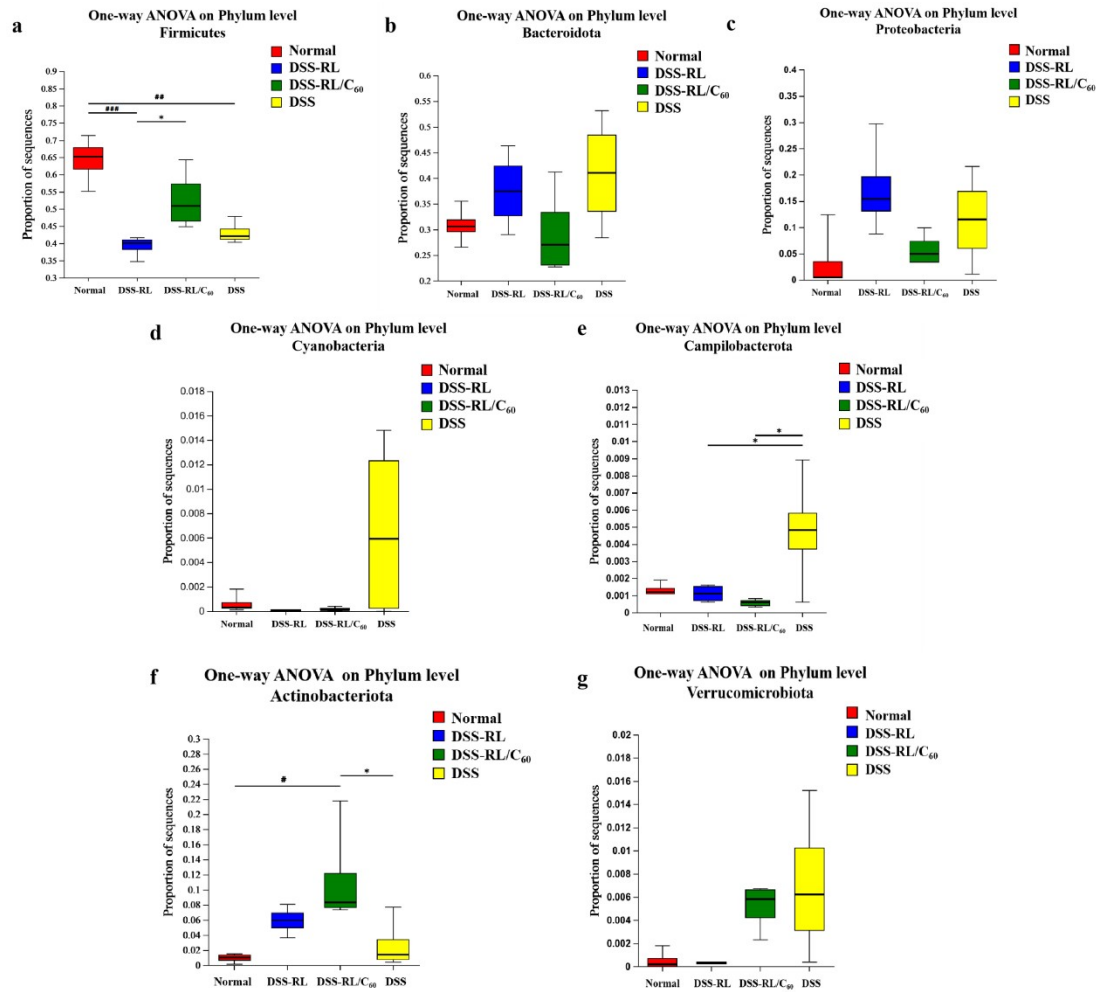


Fig. S16 Comparison of group differences in microflora at phylum level: (a) *Firmicutes*; (b) *Bacteroidota*; (c) *Proteobacteria*; (d) *Cyanobacteria*; (e) *Campilobacterota*; (f) *Actinobacteriota*; (g) *Verrucomicrobiota*. Data are shown as the mean \pm S.E.M. ($n = 4$). Statistical significance was evaluated via one-way ANOVA with Tukey Test. # $P \leq 0.05$, ## $P \leq 0.01$, ### $P \leq 0.001$ vs Normal; * $P \leq 0.05$ vs DSS.

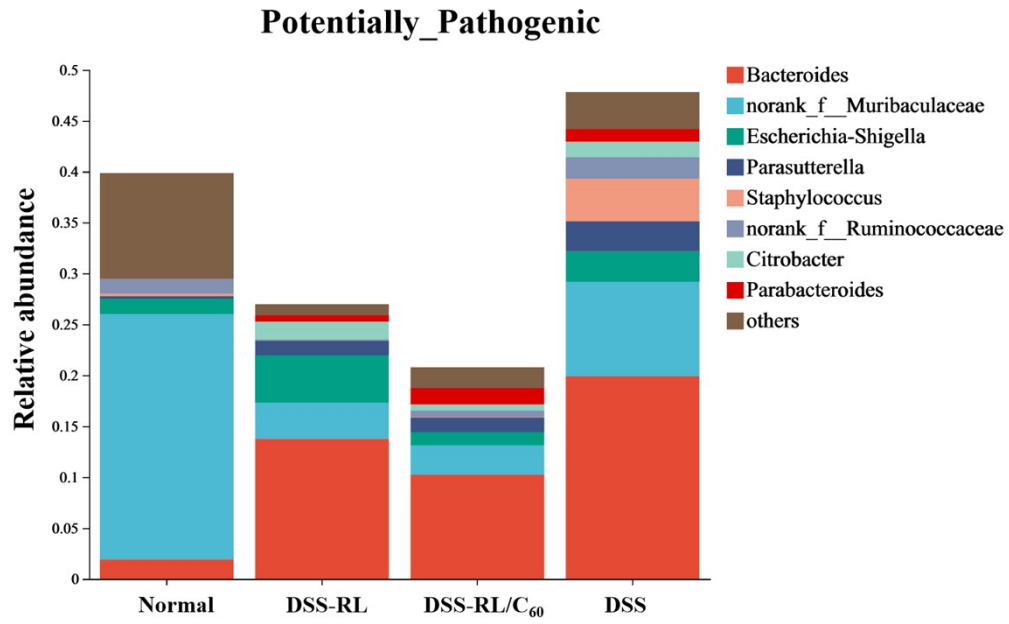


Fig. S17 Potential pathogenic histogram of microbiome in different groups predicted by BugBase.

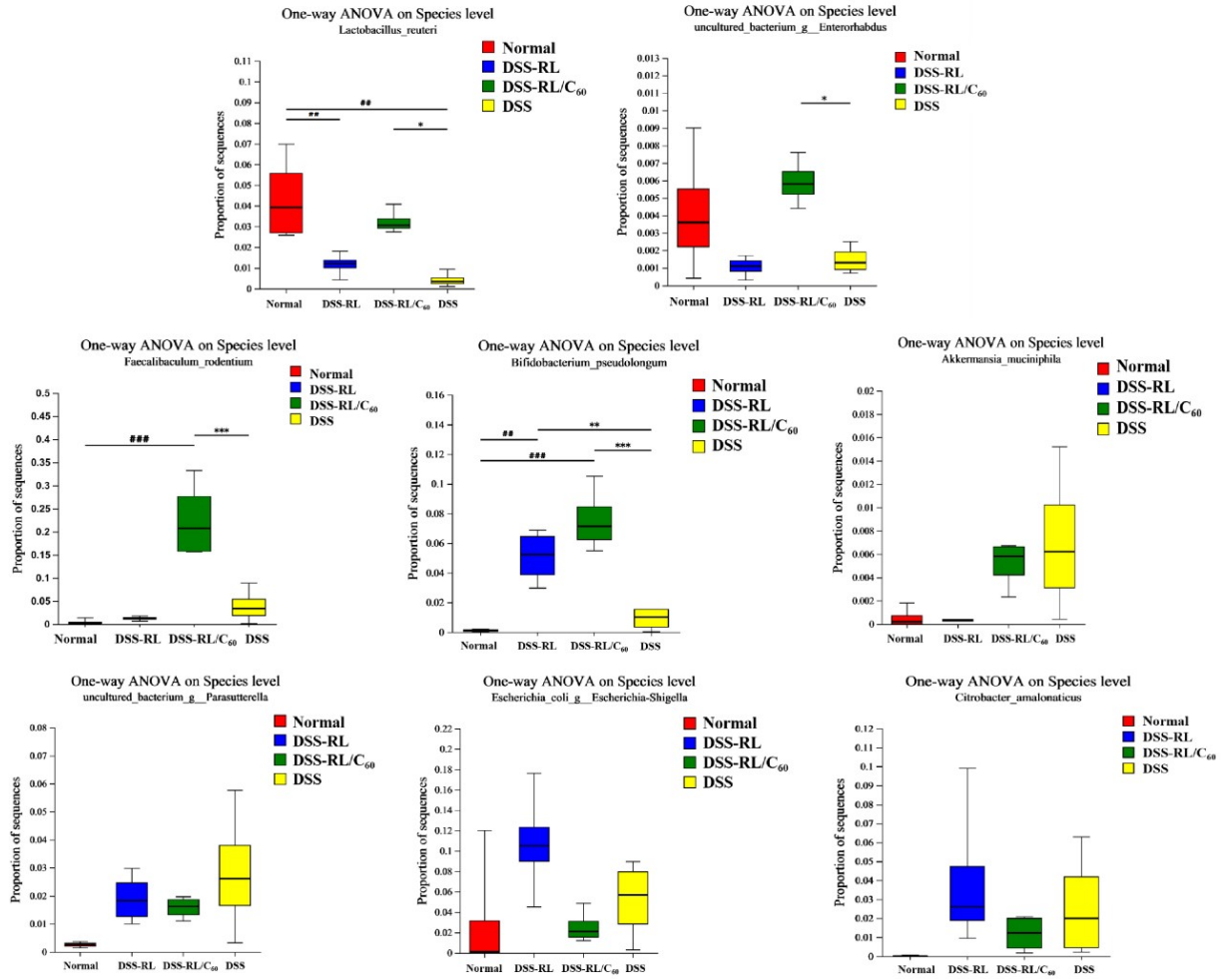


Fig. S18 RL/C₆₀ promotes probiotics colonization while suppresses harmful bacteria proliferation. Data are shown as the mean \pm S.E.M. ($n = 4$). Statistical significance was evaluated via one-way ANOVA with Tukey Test. ## $P \leq 0.01$, ### $P \leq 0.001$ vs Normal; * $P \leq 0.05$, ** $P \leq 0.01$, *** $P \leq 0.001$ vs DSS.

6. Intestinal flora-immunity relationship and its implication on UC treatment

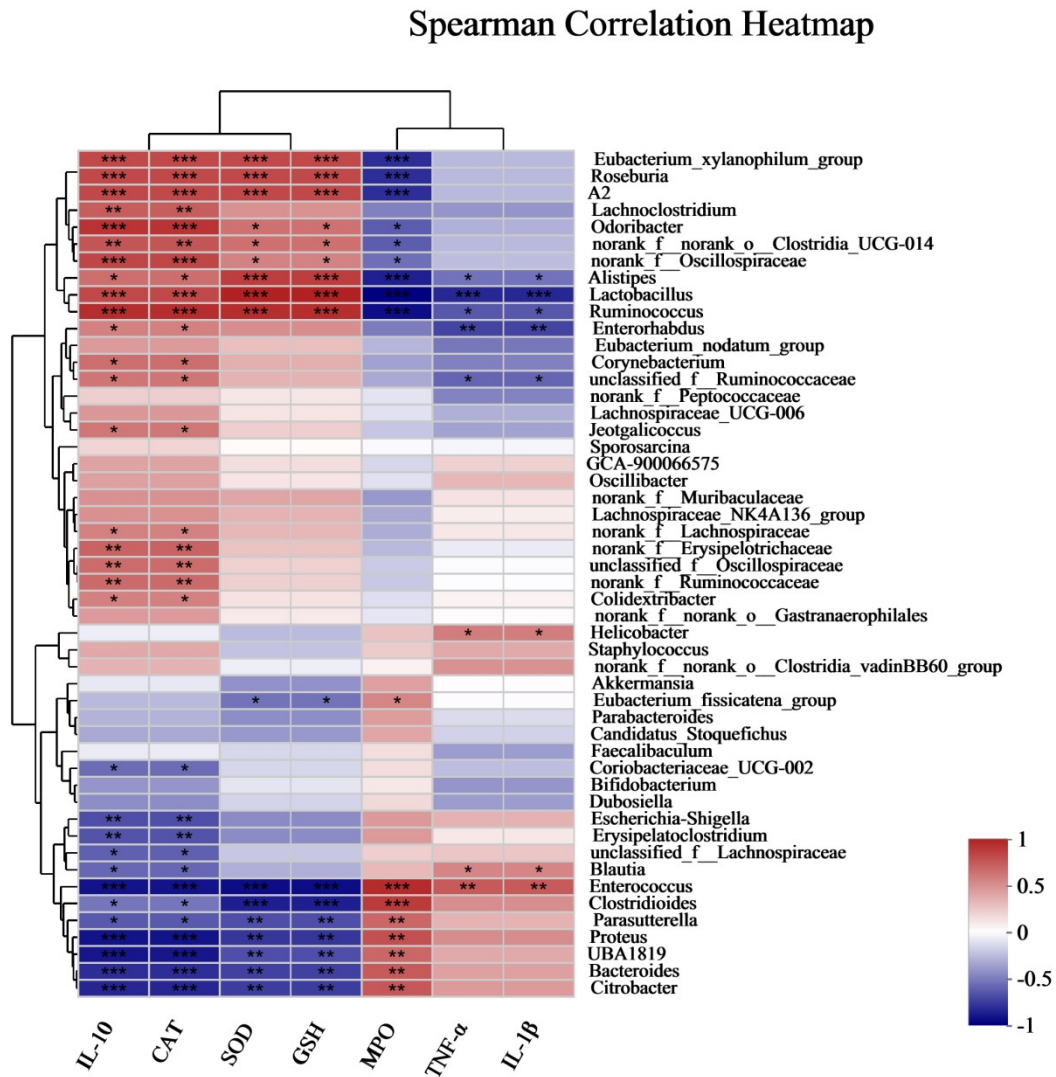


Fig. S19 Correlation heatmap of inflammatory indicators vs. microflora at genus level. Statistical significance was evaluated via one-way ANOVA with Tukey Test. * $P \leq 0.05$, ** $P \leq 0.01$, *** $P \leq 0.001$.

Table S4 SCFAs content in intestinal feces of mice in different group.

Samples	acetic acid	propanoic acid	isobutyric acid	butanoic acid	isovaleric acid	valeric acid	isohexanoic acid	hexanoic acid
Normal-1	4.450	0.730	0.092	0.657	0.074	0.068	0.015	0.019
Normal-2	9.808	0.990	0.089	0.323	0.069	0.039	0.018	0.010
Norma-3	6.420	0.918	0.115	0.990	0.109	0.157	0.022	0.014
DSS-RL-1	1.289	0.473	0.061	0.249	0.079	0.060	0.057	0.009
DSS-RL-2	2.935	1.409	0.204	0.930	0.254	0.197	0.032	0.009
DSS-RL-3	1.677	0.635	0.080	0.328	0.103	0.078	0.067	0.010
DSS-RL/C₆₀-1	8.683	0.757	0.101	0.382	0.118	0.051	0.021	0.018
DSS-RL/C₆₀-2	10.771	0.843	0.113	0.530	0.152	0.043	0.022	0.018
DSS-RL/C₆₀-3	9.589	0.727	0.100	0.475	0.137	0.041	0.016	0.019
DSS-1	1.965	0.929	0.143	0.794	0.139	0.084	0.037	0.009
DSS-2	4.523	1.313	0.162	1.002	0.205	0.158	0.026	0.010
DSS-3	4.893	1.815	0.232	1.169	0.267	0.129	0.044	0.015